CHEMISTRY OF MATERIALS
Article

Chem. Mater. **2009,** *21,* 4577–4582 4577
DOI:10.1021/cm901516b

Hollow Microporous Cerium Oxide Spheres Templated By Colloidal Silica

Nicholas C. Strandwitz[†] and Galen D. Stucky*[,†,‡]

[†]*Materials Department, University of California Santa Barbara, Santa Barbara, California 93016, and* [‡]*Department of Chemistry and Biochemistry, University of California Santa Barbara, Santa Barbara, California 93016*

Received June 2, 2009. Revised Manuscript Received July 29, 2009

We present a simple, solution-based synthetic route to hollow cerium oxide spheres. Thin layers (~12 nm) of cerium oxide are deposited onto ~200 nm silica colloids using cerium nitrate and the silica cores are subsequently removed to yield hollow spheres. The spheres are composed of ~4 nm ceria nanocrystals. Nitrogen adsorption isotherms indicate that the spheres are microporous with pore sizes of approximately 10 Å. The spheres are thermally stable to collapse and ripening up to 700 °C and are active for the catalytic combustion of carbons. The hollow ceria spheres developed in this work are attractive as building blocks for multicomponent catalysts.

1. Introduction

The development of synthetic routes to nanostructured metal oxides has received significant attention due to their promise in applications including heterogeneous catalysis and separations technology.[1,2] Significant efforts have been made to precisely control composition, structure, and hence function of inorganic materials at the nanoscale using solution-based approaches which boast potentially low cost and high yields per reactor volume.[3−5] Among different particle geometries, hollow metal oxide spheres have recently received much attention.[6] This interest is primarily fueled by the ability to confine chemicals for controlled release,[7] isolate metal nanoparticle catalysts to prevent ripening,[8,9] create high-surface area materials for batteries,[10] and create low-index-of-refraction materials.

Synthetic methods toward hollow spheres can be classified into two general categories: template and template-free strategies. Template-free routes often make use of Ostwald ripening or the Kirkendall effect. Ostwald ripening results in hollow spheres when the interior of a particle is dissolved and crystallites on the exterior of the particle grow.[10−13] The Kirkendall effect occurs when different ion diffusion rates are present during a reaction with an initially solid sphere (e.g., oxidation of cobalt metal) which are balanced by the diffusion of vacancies toward the center of the sphere.[14−17] Other template-free strategies rely on nanoparticle aggregation[18,19] or possible formation of ephemeral gas bubbles.[20,21]

Template-based syntheses of hollow spheres rely on the formation of the desired sphere component on a sacrificial template followed by template removal. An advantage of this method is that the size and the size dispersion of the final hollow spheres can be controlled by the size of the template. This process requires that the sphere component be porous to allow for template removal and the ability to selectively remove the template by calcination or dissolution. For example, monodisperse, hollow zirconia spheres were synthesized by coating silica nanoparticles with an amorphous zirconium oxide layer and the silica template was removed using sodium hydroxide.[22]

*To whom correspondence should be addressed. E-mail: stucky@chem.ucsb.edu.

(1) Ying, J. Y. *Nanostructured Materials*; Academic Press: New York, 2001.
(2) Bell, A. T. *Science* **2003**, *299*, 1688.
(3) Yang, P.; Zhao, D.; Margolese, D. I.; Chmelka, B. F.; Stucky, G. D. *Nature* **1998**, *396*, 152.
(4) Zhao, D.; Feng, J.; Huo, Q.; Melosh, N.; Fredrickson, G. H.; Chmelka, B. F.; Stucky, G. D. *Science* **1998**, *279*, 548.
(5) Schüth, F. *Angew. Chem., Int. Ed.* **2003**, *42*, 3604.
(6) Zeng, H. C. *J. Mater. Chem.* **2006**, *16*, 649.
(7) Jiang, X.; Brinker, C. J. *J. Am. Chem. Soc.* **2006**, *128*, 4512.
(8) Arnal, P. M.; Comotti, M.; Schuth, F. *Angew. Chem., Int. Ed.* **2006**, *45*, 8224.
(9) Huang, X.; Guo, C.; Zuo, J.; Zheng, N.; Stucky, G. D. *Small* **2009**, *5*, 361.
(10) Lou, X. W.; Wang, Y.; Yuan, C.; Lee, J. Y.; Archer, L. A. *Adv. Mater.* **2006**, *18*, 2325.
(11) Chang, Y.; Teo, J. J.; Zeng, H. C. *Langmuir* **2005**, *21*, 1074.
(12) Yang, H. G.; Zeng, H. C. *J. Phys. Chem. B* **2004**, *108*, 3492.
(13) Li, J.; Zeng, H. C. *J. Am. Chem. Soc.* **2007**, *129*, 15839.
(14) Liu, J.; Xue, D. F. *Adv. Mater.* **2008**, *20*, 2622.
(15) Yin, Y. D.; Rioux, R. M.; Erdonmez, C. K.; Hughes, S.; Somorjai, G. A.; Alivisatos, A. P. *Science* **2004**, *304*, 711.
(16) Yin, Y. D.; Erdonmez, C. K.; Cabot, A.; Hughes, S.; Alivisatos, A. P. *Adv. Funct. Mater.* **2006**, *16*, 1389.
(17) Shevchenko, E. V.; Bodnarchuk, M. I.; Kovalenko, M. V.; Talapin, D. V.; Smith, R. K.; Aloni, S.; Heiss, W.; Alivisatos, A. P. *Adv. Mater.* **2008**, 9999.
(18) Li, L.; Chu, Y.; Liu, Y.; Dong, L. *J. Phys. Chem. C* **2007**, *111*, 2123.
(19) Mao, L.-j.; Liu, C.-y.; Li, J. *J. Mater. Chem.* **2008**, *18*, 1640.
(20) Naik, S. P.; Chiang, A. S. T.; Thompson, R. W.; Huang, F. C. *Chem. Mater.* **2003**, *15*, 787.
(21) Yan, A.; Liu, X.; Yi, R.; Shi, R.; Zhang, N.; Qiu, G. *J. Phys. Chem. C* **2008**, *112*, 8558.
(22) Arnal, P. M.; Weidenthaler, C.; Schuth, F. *Chem. Mater.* **2006**, *18*, 2733.

Published on Web 09/01/2009

The silica-based templating of polymer,[23] carbon,[24−26] SnO_2,[27] ZrO_2,[22,25] and Pd[28] hollow spheres of have been reported.

Because cerium oxide is catalytically active, a common support for a number of nanoparticle catalysts,[29−31] generally nontoxic, and abundant, hollow spheres of cerium oxide are desirable. Hollow cerium oxide spheres have been prepared by templating aqueous cerium precursor solutions with large[32] (>10 um) and small[33] (~100−200 nm) polystyrene beads. Pore size distributions and temperature stability of the CeO_2 spheres were not reported. In the case of the 100−200 nm hollow spheres, many of the spheres were broken suggesting that the process was not robust.[33]

Here, we report the synthesis and characterization of porous cerium oxide coated silica particles and hollow cerium oxide spheres. The synthetic conditions for the formation of the porous cerium oxide coatings on silica templates were investigated along with the temperature stability, porosity, and phase evolution of the hollow spheres.

2. Experimental Section

2.1. Materials. All materials were used as received including ethylene glycol (BDH, 99%), cerium(III) nitrate hexahydrate (99%, Sigma-Aldrich), tetraethylorthosilcate (TEOS, Sigma-Aldrich), ammonium hydroxide (29%, ACS grade), ethanol (200 proof, Gold Shield), sodium hydroxide (ACS grade), and cerium(IV) oxide nanopowder (Sigma-Aldrich). Deionized water was used for all manipulations.

2.2. SiO_2 Template Particles. Ethanol (280 mL) was mixed with TEOS (8 mL). While stirring, a mixture of water (56 mL) and ammonium hydroxide (8.4 mL) was added to the TEOS/ethanol solution at room temperature in a 500-mL Erlenmeyer flask at room temperature (20 °C), and the top was sealed with Parafilm. This mixture was stirred for 24 h, then successively centrifuged (8200 RCF, 9 min) and redispersed in water and ethanol, and then finally dried at 65 °C for 6 h. For the silica pretreatment studies, the same washing procedure was followed, except the silica was dried under ambient conditions or for longer periods of time at 65 °C.

2.3. SiO_2@CeO_2 and @CeO_2 Hollow Spheres. Typically, 300 mg of dried SiO_2 templates were dispersed in 43 mL of ethylene glycol with ultrasonication. Cerium nitrate (1 M, 2.25 mL) was added and the mixture was stirred for 10 min. This mixture was heated to 130 °C for 15 h in a 500 mL round-bottom flask sealed with a glass stopper secured with a metal clip. *Caution! The presence of water should be carefully considered to avoid explosion.* Alternatively, a Teflon-lined stainless steel reactor was utilized for the ceria deposition at filling fractions less than 75%. The reaction vessel was then cooled to room temperature and the SiO_2@CeO_2 particles were isolated by centrifugation (12,500 RCF, 10 min) and washed with ethanol. To remove the silica cores, the SiO_2@CeO_2 particles were dispersed in 5 M NaOH for 2 days at room temperature (20 °C) in a 50 mL polypropylene centrifuge tube, with a fresh solution of NaOH (10 mL) exchanged after 1 day. The hollow @CeO_2 spheres were isolated by successive centrifugation (3200 RCF, 10 min), redispersed in water and then ethanol, and dried in air.

Scheme 1. Process Flow for Forming Hollow CeO_2 Spheres.

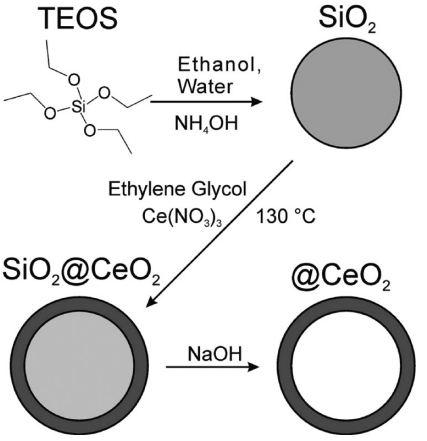

2.4. Characterization. Transmission electron microscopy (TEM) was performed on a FEI Tecnai G2 Sphera Microscope operating at 200 kV. Size distributions of the silica templates were obtained by measuring the diameters of >100 particles from TEM images using commercial software (ImageJ). The CeO_2 wall thicknesses were measured similarly by TEM. In this case, the wall was assumed to begin at the outer edge of a sphere and terminate at the easily observed CeO_2−SiO_2 interface. Scanning electron microscopy (SEM) was performed on a FEI XL30 Sirion FEG Digital Electron Scanning Microscope operating at 12 kV. X-ray diffraction (XRD) was performed using a Bruker D8 advance for temperature-dependent analysis and a Phillips XPERT powder diffractometer. ^{29}Si MAS NMR was performed on a Bruker AVANCE500 WB spectrometer (500 MHz, 11.7 T). Thermogravimetric analyses were conducted on a Mettler TGA/sDTA851e at a heating rate of 5 °C/min under air (40 sccm) and nitrogen (30 sccm) flow. A Micromeritics ASAP 2000 was used to acquire N_2 sorption isotherms. Micromeritics 2020 V3.03 software was used to calculate specific surface areas and pore size distributions. For the Horvath−Kawazoe method, the Saito−Foley option for cylindrical pores was used.

3. Results and Discussion

3.1. Synthesis and Structural Evolution. The hollow ceria spheres (denoted @CeO_2) were formed by the silica-templating approach (Scheme 1). First, silica spheres were synthesized via a modified Stöber method,[34] subsequently washed with water and ethanol, and then subject to a mild thermal treatment. Next, the silica particles were coated with cerium oxide via a solvothermal reaction in ethylene glycol[35] and cerium nitrate at 130 °C forming

(23) Kamata, K.; Lu, Y.; Xia, Y. *J. Am. Chem. Soc.* **2003**, *125*, 2384.
(24) Kim, J. Y.; Yoon, S. B.; Yu, J. S. *Chem. Commun.* **2003**, 790.
(25) Arnal, P. M.; Schuth, F.; Kleitz, F. *Chem. Commun.* **2006**, 1203.
(26) Yoon, S. B.; Sohn, K.; Kim, J. Y.; Shin, C. H.; Yu, J. S.; Hyeon, T. *Adv. Mater.* **2002**, *14*, 19.
(27) Lou, Xiong W.; Yuan, C.; Archer, L. A. *Small* **2007**, *3*, 261.
(28) Kim, S. W.; Kim, M.; Lee, W. Y.; Hyeon, T. *J. Am. Chem. Soc.* **2002**, *124*, 7642.
(29) Si, R.; Flytzani-Stephanopoulos, M. *Angew. Chem., Int. Ed.* **2008**, *47*, 2884.
(30) Mikulova, J.; Barbier, J.; Rossignol, S.; Mesnard, D.; Duprez, D.; Kappenstein, C. *J. Catal.* **2007**, *251*, 172.
(31) Trovarelli, A. *Catalysis by Ceria and Related Materials*; Imperial College Press: London, 2002.
(32) Kartsonakis, I. A.; Liatsi, P.; Daniilidis, I.; Kordas, G. *J. Am. Ceram. Soc.* **2008**, *91*, 372.
(33) Shchukin, D. G.; Caruso, R. A. *Chem. Mater.* **2004**, *16*, 2287.
(34) Stober, W.; Fink, A.; Bohn, E. *J. Colloid Interface Sci.* **1968**, *26*, 62.
(35) Liang, X.; Wang, X.; Zhuang, Y.; Xu, B.; Kuang, S. M.; Li, Y. D. *J. Am. Chem. Soc.* **2008**, *130*, 2736.

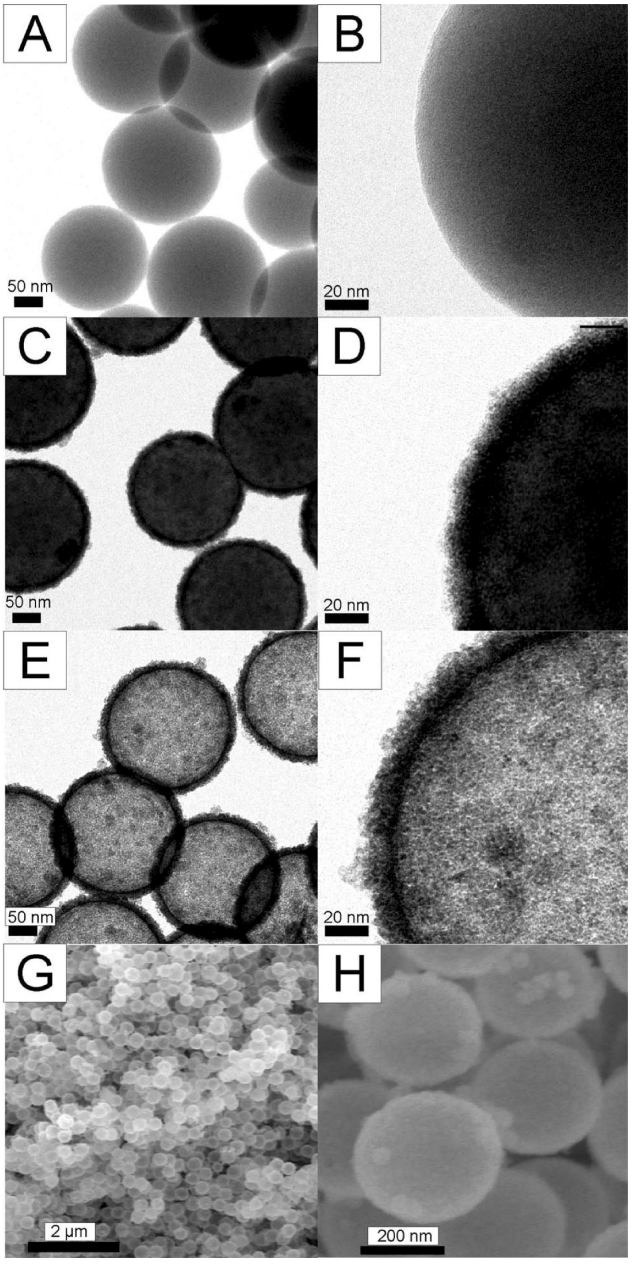

Figure 1. TEM images of SiO_2 templates (A, B), SiO_2@CeO_2 (C, D), @CeO_2 (E, F) spheres. SEM images of @CeO_2 spheres (G, H).

SiO_2@CeO_2 (core@shell) particles. The core@shell particles were isolated by centrifugation. Finally, the SiO_2 cores were chemically etched with NaOH yielding hollow @CeO_x spheres.

The silica template particles had an average diameter of 203 ± 18 nm (Figure 1A and B) and exhibited a BET (Brunauer−Emmett−Teller) specific surface area of 14 m^2/g (Table 1). The calculated surface area of nonporous silica spheres of the same diameter is ~12 m^2/g, suggesting that the silica templates are nonporous. The pore volume and micropore volume calculated from the absorption isotherm were 0.06 and 0.003 cm^3/g, respectively (Table 1). The chemical composition of the silica templates, and the effects of the mild thermal treatment will be discussed below.

After coating the SiO_2 templates with ceria, the interface between the silica and ceria can be clearly observed

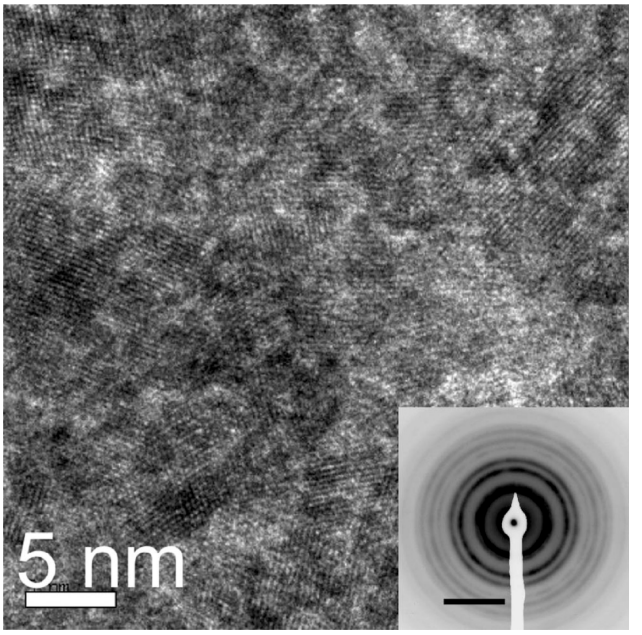

Figure 2. High magnification TEM image with visible lattice fringes and (inset) selected area electron diffraction pattern of a single hollow sphere (inset scalebar = 6 nm^{-1}).

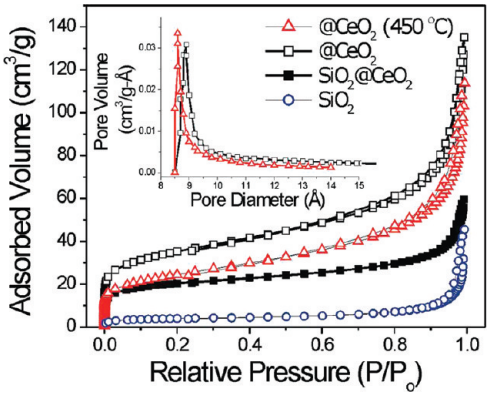

Figure 3. Nitrogen sorption isotherms for the annealed @CeO_2 (open triangles), @CeO_2 (open squares), SiO_2@CeO_2 particles (closed squares), and SiO_2 template spheres (open circles). (inset) Horvath−Kawazoe pore size distribution for annealed and as-synthesized @CeO_2.

using TEM due to the differences in morphology and cation atomic number between the two phases (Figure 1C and D). The CeO_2 coatings were nanocrystalline as-synthesized with a crystallite size of approximately 2−5 nm by TEM analysis and approximately 4 nm as calculated by XRD peak-broadening using the Scherrer formula.[36] All peaks could be indexed to cubic CeO_2. The average thickness of the CeO_2 coatings was 12 ± 3 nm as measured by TEM. Several small, free ceria nanoparticles were present; however, most of the ceria was bound to the SiO_2 templates. The presence of these small ceria spheres not bound to the silica templates is attributed to nucleation of ceria crystallites *in solution* which *remain in solution*.

Nitrogen adsorption isotherms indicate microporosity in the SiO_2@CeO_2 particles by the steep rise in adsorbed

(36) Patterson, A. L. *Phys. Rev.* **1939**, *56*, 978.

Table 1. Properties of the SiO_2, SiO_2@CeO_2, and @CeO_2 Particles

material	S_{BET} (m^2/g)	pore diameter (Å)	micropore volume (cm^3/g)	total pore volume (cm^3/g)
SiO_2	14.1		0.003	0.06
SiO_2@CeO_2	70.5		0.022	0.09
@CeO_2	123	10	0.028	0.20
@CeO_2 (450 °C)	85.9	8	0.014	0.17

volume at low pressures (Figure 3), in which case BET surface areas are not necessarily accurate.[37] However, BET data provide an estimation and yield trends of specific surface area. The BET surface area of the SiO_2@CeO_2 particles was 70.5 m^2/g. Considering the mass of the SiO_2 templates and the mass increase due to the CeO_2 coating, the calculated specific surface area contribution from the CeO_2 coatings is 139 m^2/g. The pore volume and micropore volume increased over those of the SiO_2 templates to 0.09 and 0.022 cm^3/g, respectively. Considering the mass or each phase, the contribution to the pore volume and micropore volume of the CeO_2 coatings alone is calculated to be 0.126 and 0.044 cm^3/g.

The spherical morphology of CeO_2 crystallites was maintained after removal of the silica template with NaOH prior to annealing or calcination. The ability to remove the SiO_2 cores is conclusive evidence that the ceria coatings have a porous structure. A significant increase in contrast is observed by TEM between the CeO_2 layer and the now-hollow interior (Figure 1E and F). The presence of lattice fringes in TEM images taken through the center of a single sphere confirms that the shells are comprised of small ceria nanocrystals (1−4 nm) which are randomly oriented (Figure 2 and the Supporting Information). Selected area electron diffraction (SAED) on a single sphere shows rings corresponding to randomly oriented ceria crystallites. The rings observed in SAED and measurements of the lattice fringes observed by TEM are indexed as cubic CeO_2.

Although no other crystalline phases were observed in the hollow spheres, Si was detected by TEM EDS (energy dispersive X-ray spectroscopy) at a concentration of 3.1 wt %. Additional leaching steps (up to 4 days with a fresh NaOH solution each day along with heating to 100 °C) did not decrease the amount of silica observed. This is consistent with other reports for deposition of ZrO_2 on silica.[22] It is likely that the ceria-bound Si is not removed and that Si−O−Ce bonds are present, as isolated SiO_2 is readily dissolved with NaOH. This observation provides evidence that a chemical reaction occurs between the cerium oxide particles or cerium precursor during ceria deposition.

The BET surface area of the hollow CeO_2 spheres was 123 m^2/g, similar to the value estimated above. The approximate contribution of the external surfaces (outer surface and inner surface of the spheres) based on the spherical geometry and bulk density of CeO_2 of 7.65 g/cm^3 is approximately 17 m^2/g. Therefore, a significant contribution to the specific surface area (105 m^2/g) is attributed to surface roughness and internal surface area of the CeO_2. A logarithmic plot of the adsorption isotherm shows a rapid rise in the adsorbed volume at low relative pressures which indicates microporosity in the hollow spheres.[37] Horvath−Kawazoe (HK) with Saito−Foley (cylindrical) geometry analysis of the isotherm indicates an approximate pore size distribution centered at 10 ± 2 Å. The pore size distribution was also calculated using the density functional theory (DFT) method, which yields a peak at 9 Å along with smaller peaks from 16 to 200 Å (Supporting Information).

Using a strictly geometric argument, close-packing of 5-nm spherical particles yields nonspherical interstitial spaces of approximately 8 Å, which is similar in size to the average pore size by HK and DFT analyses. Here, we note, however, that there is no evidence of close-packing of ceria crystallites and that the distribution of ceria particles appears to be random. The presence of larger pores (50−200 Å) by DFT analysis may be due to the inherent presence of interstitial space between the hollow spheres during the sorption measurements, which should yield a broad range of pore sizes in this size range. HK analyses were, however, only applied to the low relative pressure regime (<0.2) and therefore do not show evidence of pores in this size range. TEM images, the qualitative shape of the sorption isotherm, along with DFT and HK analyses together provide strong evidence for a disordered pore structure with pore diameters of approximately 10 Å.

After annealing the hollow spheres at 450 °C, no change in the XRD pattern or TEM images are observed. The BET specific surface area and average pore size decrease to ∼70 m^2/g and 9 ± 2 Å, respectively. The decrease in specific surface area is likely due to a relaxation or slight sintering of the nanocrystals which comprise the shell, decreasing the available surface area between the nanocrystals. Similarly, a decrease in pore volume and micropore volume are observed (Table 1).

The temperature-induced structural evolution and stability of the hollow spheres are highly important parameters for catalytic applications. Crystallite growth by Ostwald ripening is expected to coincide with collapse of the spherical structure. We therefore monitored the XRD pattern of the @CeO_2 spheres at various temperatures between 30 and 850 °C (Supporting Information). Using XRD peak-broadening as a metric to monitor average crystallite size, we have plotted crystallite size vs temperature (Figure 4). The small crystallite size (∼4 nm) of the as-synthesized CeO_2 shells is constant up to ∼700 °C. At temperatures greater than 750 °C, the crystallite size rapidly increases. Similarly, TEM images indicate that the spheres are stable to collapse up to 700 °C. However,

(37) Webb, P. A.; Orr, C. *Analytical Methods in Fine Particle Technology*; Micromeritics Instrument Corp., Norcoss, GA, 1997.

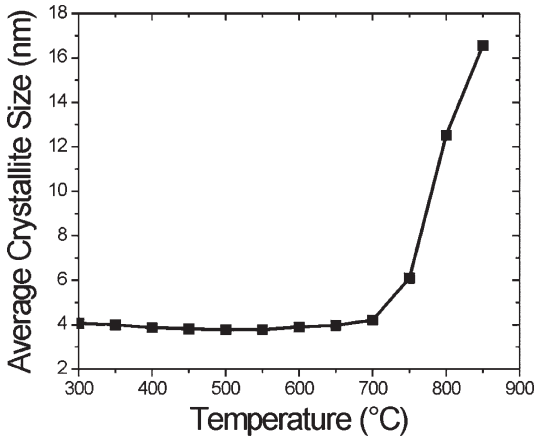

Figure 4. Approximate crystallite size of CeO_2 hollow spheres as a function of temperature calculated by Scherrer analysis of the XRD pattern (see the Supporting Information).

at temperatures above 750 °C, significant crystal growth occurs accompanied by the collapse of the hollow sphere geometry (Supporting Information).

3.2. Formation Mechanism. Mild thermal treatment of the SiO_2 template particles after the modified-Stöber synthesis was found to be essential to the formation of conformal CeO_2 coatings. After repeated washing and isolation by centrifugation, three treatments of SiO_2 templates were examined prior to CeO_2 coating: drying at room temperature for 24 h, drying at 65 °C for 6 h, and drying at 65 °C for 24 h. Attempts to coat the silica sample dried at room temperature resulted in sparse, submonolayer coatings and many uncoated SiO_2 templates (Supporting Information). Attempts to coat the sample dried at 65 °C for 25 h resulted in larger (20 nm), isolated CeO_2 particles decorated on the SiO_2 surface. Only drying the templates at 65 °C for 3−8 h resulted in a conformal coating of nanocrystalline CeO_2 under our reaction conditions.

To investigate the dependence of the ceria coating on SiO_2 pretreatment, we conducted solid state ^{29}Si NMR and FTIR analyses of the three SiO_2 samples prior to ceria deposition. In ^{29}Si NMR, three peaks were visible corresponding to Q_2 $(SiO)_2\mathbf{Si}(OH)_2$, Q_3 $(SiO)_3\mathbf{Si}(OH)$, and Q_4 $(SiO)_4\mathbf{Si}$ silica species (Figure 5A). A progressive increase in integrated value of the Q_4 peaks relative to Q_2 and Q_3 peaks is observed with more prolonged heat treatment. The relative increase in the Q_4 peak indicates an increasing degree of condensation of the silica network. The concentration of silanol groups in the SiO_2 templates will decrease with increasing thermal treatment as the condensation reaction typically eliminates two silanol groups forming a siloxane bond.

FTIR spectra indicate a lack of free (i.e., non-hydrogen bonded) silanol groups in the SiO_2 which are expected to occur at 3737 cm^{-1} (Figure 5B and C).[38] A broad absorption feature is observed from 3680 to 2450 cm^{-1}

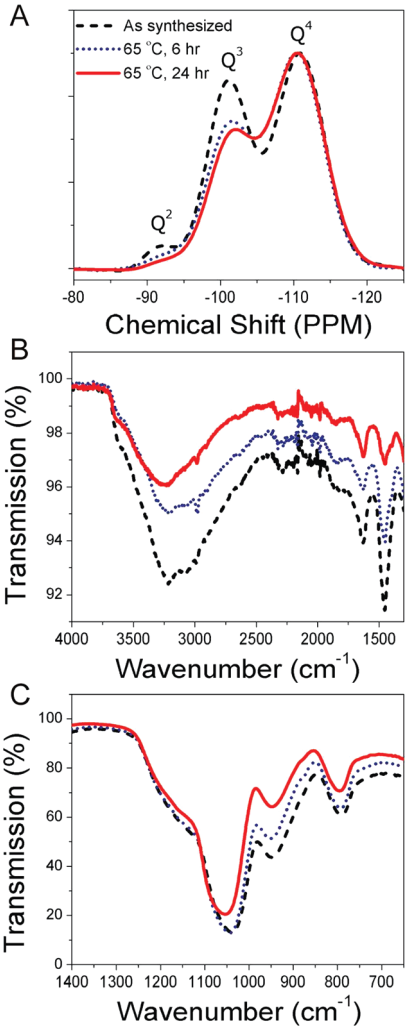

Figure 5. ^{29}Si NMR (A) and FTIR (B, C) spectra of silica template particles as synthesized (black, dashed line) after thermal treatment at 65 °C for 6 h (blue, dotted line) and 24 h (red, solid line).

which is attributed to water and H-bonded silanols.[39−41] The narrow absorption band at 2980 cm^{-1} is due to CH stretching of ethoxy groups and/or ethanol.[41] Absorption due to water is observed at 1630 cm^{-1}. Absorption at 1460 cm^{-1} is attributed to CH stretching and/or the presence of NH_4^+ ions.[42] Structural SiOSi absorption bands are observed at 1050 and 790 cm^{-1}.[43] Another absorption band due to silanols and possibly SiO^- groups is present at 950 cm^{-1}.[43]

Thermal treatment at 65 °C induces a significant decrease in the intensity of the silanol bands (3680−2450 and 950 cm^{-1}) and is indicative of partial water loss and/or partial condensation of silanol groups. Absorption bands due to the presence of CH groups (2980 cm^{-1}) are decreased, but still present. Some ethoxy groups and/or ethanol are therefore removed by thermal treatment.

(38) Barby, D. Silicas. In *Characterization of powder surfaces with special reference to pigments and fillers*; Parfitt, G. D.; Sing, K. S. W., Eds.; Academic Press Inc. Ltd.: London, 1976; p 353.
(39) Kondo, S.; Muroya, M.; Fujii, K. *Bull. Chem. Soc. Jpn.* **1974**, *47*, 553.
(40) Mondragon, M. A.; Castano, V. M.; Garcia, J.; Tellez, C. A. *Vib. Spectrosc.* **1995**, *9*, 293.
(41) Costa, C. A. R.; Leite, C. A. P.; Galembeck, F. *J. Phys. Chem. B* **2003**, *107*, 4747.
(42) Burneau, A.; Barres, O.; Gallas, J. P.; Lavalley, J. C. *Langmuir* **1990**, *6*, 1364.
(43) Matos, M. C.; Ilharco, L. M.; Almeida, R. M. *J. Non-Cryst. Solids* **1992**, *147*, 232.

Similarly, a decrease in absorbance at 1460 cm^{-1} is indicative of loss of some NH_4^+ or ethoxy groups. Finally, a shift in the SiOSi absorption bands is also observed, which indicates structural change, such as further condensation.

Silanol groups likely play a major role in the surface charge as well as in potential binding sites for ceria precursors. Our data clearly show the need for a mild thermal treatment for conformal ceria coatings. We speculate that the mild thermal treatments are necessary for several reasons. First, the removal of some NH_4^+ ions or ethoxy groups may be important to allow for ceria deposition on the silica surface. The decrease in the FTIR absorption band at 1460 cm^{-1} upon thermal treatment supports this claim. Second, specific types of silanol groups may be needed for ceria deposition on the surface. Silanols exist in a variety of H-bonded environments in alkoxy-derived (i.e., precipitated) silicas as indicated by the broad absorption feature from 3680 to 2450 cm^{-1}.[39] The structure and abundance of the silanol groups change even under these mild thermal treatments as indicated by the change in this IR absorption feature and the relative ratio of Q_4 silica relative to Q_3 in ^{29}Si NMR. Finally, more-extensive temperature treatments (e.g., >20 h at 65 °C) result in nonuniform ceria coverage on the SiO_2 possibly due to a decreased density of surface silanols (converted to siloxane) or an overall unfavorable silanol environment for the deposition of ceria. Although FTIR and NMR measurements yield information regarding the surface and bulk of the templates, we expect that these measurements indicate similar changes on the template surface, where ceria deposition occurs.

The formation of the ceria coatings likely proceeds via nanocrystal assembly or via nucleation of nanocrystals directly on the SiO_2 surface. Time-resolved TEM studies of the process show the growth of the CeO_2 coating (Supporting Information). Because the pH of the solution is near neutral or mildly acidic, the SiO_2 template particles are negatively charged and are able to attract Ce^{3+} cations. Cerium oxide formation may occur by the decomposition of the cerium salt into the oxide, as in other reports.[35,44] Notably, here we use significantly lower temperatures (130 °C rather than 180 °C). The presence of the negative SiO_2 surface may increase the local concentration of Ce^{3+} allowing for a lower-temperature nucleation threshold. In situ time-resolved TEM studies might provide new evidence regarding the precise mechanism.

3.3. Catalytic Combustion. For applications in catalysis, it is critical that coke is combusted while maintaining the spherical nanocrystalline structure. We examined thermogravimetry analysis (TGA) traces of hollow ceria spheres mixed with 25% carbon (Fuel Cell Store). When no spheres were present, the carbon is thermally stable and only a mass loss of ~2% is observed at 600 °C (Figure 6). When ceria spheres are mixed with the carbon, a mass loss corresponding to 100% of the carbon is observed at 575 °C. We compared the hollow ceria spheres to commercially available ceria nanocrystals (1−60 nm diameter, Sigma-Aldrich) which showed similar performance to the @CeO_2 particles. Electron microscopy after the combustion reaction revealed that the spherical morphology of the hollow spheres remained largely intact, although some structural collapse had occurred (Supporting Information). The catalytic activity of the @CeO_2 particles is thus favorable for decoking in catalysis applications; however, their long-term stability must be further investigated along with other relevant catalytic reactions.[31]

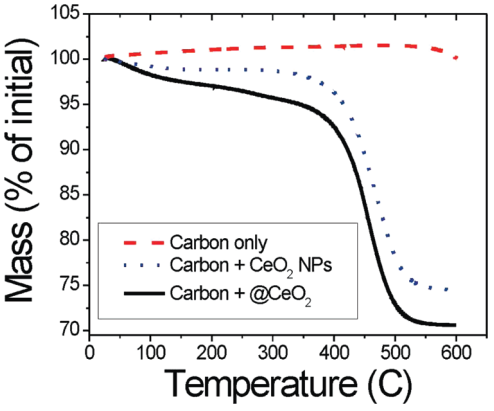

Figure 6. Thermogravimetric analysis of carbon mixed with hollow ceria spheres (solid black line), commercially available ceria (dotted blue line), and carbon alone (dashed red line).

4. Conclusion

We have demonstrated a simple synthetic strategy for the formation of hollow ceria spheres templated by colloidal silica. A high yield of thermally stable hollow spheres was obtained by solvothermal reaction with cerium nitrate. Mild thermal treatment was found to be essential to tuning the interactions between Ce^{3+} precursor and the SiO_2 template surface. As techniques for the encapsulation of noble-metal nanoparticles (e.g., Au) in silica are well-developed,[9,45] the strategy presented here can be readily extended for their encapsulation inside the porous ceria spheres. Thus, this synthetic strategy toward hollow spheres constitutes an important building block for multicomponent nanoparticle catalysts.

Acknowledgment. We gratefully acknowledge funding from Corning, Inc. and fruitful discussions with its scientists. This work made use of MRL Central Facilities supported by the MRSEC program of the National Science Foundation under Award No. DMR05-20415. We thank Alan Kleiman for help with the high-temperature XRD measurements and Dr. Jan P. Löfvander for assistance with TEM.

Supporting Information Available: Additional TEM images, high-temperature XRD patterns, time-resolved TEM images, and DFT pore size analysis. This material is available free of charge via the Internet at http://pubs.acs.org.

(44) Ho, C.; Yu, J. C.; Kwong, T.; Mak, A. C.; Lai, S. *Chem. Mater.* **2005**, *17*, 4514.

(45) Liz-Marzan, L. M.; Mulvaney, P. *J. Phys. Chem. B* **2003**, *107*, 7312.